TOP MASS MEASUREMENT AT CMS*

Markus Duda

III. Physikalisches Institut B, RWTH Aachen
Otto-Blumenthal-Straße, D-52074 Aachen, Germany

(Received November 15, 2006)

Given the big cross section for $t\bar{t}$ production in proton-proton collisions at 14 TeV, the LHC with its high luminosity will be, among others, a top factory, allowing a precision measurement of the top quark mass. Based on a detailed simulation of the CMS detector, the following top mass reconstruction accuracies are possible in the respective final states with the present knowledge of experimental and theoretical uncertainties.

$$\begin{array}{lcl}
\Delta m_t(\mathrm{dileptonic}, 1\,\mathrm{fb}^{-1}) & = & \pm 1.5\,(\mathrm{stat.}) \pm 2.9\,(\mathrm{syst.})\,\mathrm{GeV}/c^2 \\
\Delta m_t(\mathrm{semileptonic}, 1\,\mathrm{fb}^{-1}) & = & \pm 0.7\,(\mathrm{stat.}) \pm 1.9\,(\mathrm{syst.})\,\mathrm{GeV}/c^2 \\
\Delta m_t(\mathrm{fully\ hadronic}, 1\,\mathrm{fb}^{-1}) & = & \pm 0.6\,(\mathrm{stat.}) \pm 4.2\,(\mathrm{syst.})\,\mathrm{GeV}/c^2 \\
\Delta m_t(\mathrm{dileptonic}, 10\,\mathrm{fb}^{-1}) & = & \pm 0.5\,(\mathrm{stat.}) \pm 1.1\,(\mathrm{syst.})\,\mathrm{GeV}/c^2 \\
\Delta m_t(\mathrm{semileptonic}, 10\,\mathrm{fb}^{-1}) & = & \pm 0.2\,(\mathrm{stat.}) \pm 1.1\,(\mathrm{syst.})\,\mathrm{GeV}/c^2 \\
\Delta m_t(J/\Psi, 20\,\mathrm{fb}^{-1}) & = & \pm 1.2\,(\mathrm{stat.}) \pm 1.5\,(\mathrm{syst.})\,\mathrm{GeV}/c^2
\end{array}$$

A combined top mass accuracy of $\mathcal{O}(1\,\mathrm{GeV}/c^2)$ for $10 - 20\,\mathrm{fb}^{-1}$ of well-understood CMS data will be feasible.

PACS numbers: 14.65.Ha

1. Introduction

At LHC top quarks will be produced dominantly as $t\bar{t}$ pairs with their production cross section calculated to be 830 pb [1] at NLO. Contrary to Tevatron the dominant production mechanism at LHC is gluon–gluon fusion accounting for about 90% of the $t\bar{t}$ events, while quark–antiquark annihilation only contributes about 10%. According to the Standard Model the top quark decays almost exclusively to a b quark and a W boson. The decays of the $t\bar{t}$ system are then classified according to the decays of the W^+W^- system as dileptonic, semi-leptonic or fully hadronic. Neglecting higher order corrections, the branching ratios of those three decay channels are $9/81$

* Presented at the "Physics at LHC" Conference, Kraków, Poland, July 3–8, 2006.

(11.1%) for the dileptonic, 36/81 (44.4%) for the semi-leptonic and 36/81 (44.4%) for the fully hadronic final state.

2. Dileptonic final states

The dileptonic channel offers an easily selectable and clean final state, but the presence of two neutrinos prevents a direct reconstruction of the top quark mass. However, the event kinematic retains a large sensitivity to the top mass. The method presented here is discussed in more detail in [2].

Events are selected using the single- and dilepton trigger, and then requiring at least two isolated opposite-sign leptons with $p_T > 20$ GeV/c. Fig. 1 shows the invariant mass of the two highest-p_T lepton candidates, a cut around the visible Z mass peak is used to remove the contamination due to Z+jets events. Selected events must also contain at least two b-tagged jets with $p_T > 30$ GeV/c, using the CMS combined b-tagging algorithm [3]. An upper cut on the number of high-p_T jets is used to suppress the other $t\bar{t}$ final states. Finally, a $E_T^{\rm miss} > 40$ GeV selection cut reflects the presence of two neutrinos in the final state of signal events. This selection already achieves a S/B of 7.3 with the other $t\bar{t}$ channels dominating the remaining background.

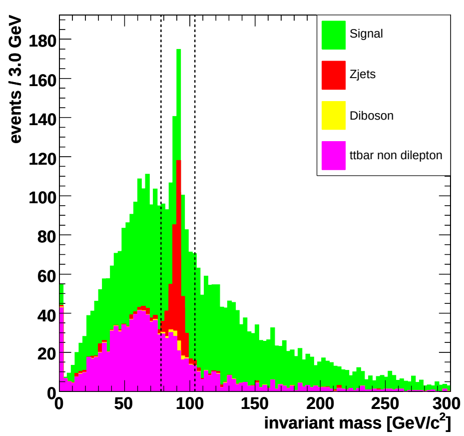

Fig. 1. Invariant mass distribution of the two highest-p_T lepton candidates, indicated is the cut window to remove Z+jets events.

The event kinematics of the dileptonic $t\bar{t}$ decay channel yield an underconstrained equation system due to the two undetected neutrinos in the final state. Using the constraints of momentum balance in the transverse plane, the known m_W and the equality of both top quark masses, the event kinematics can be written as a fourth order polynomial with the top mass as a parameter. For each selected event, top mass values in the range

$100\,\mathrm{GeV}/c^2 \leq m_t \leq 300\,\mathrm{GeV}/c^2$ are tested in $1\,\mathrm{GeV}/c^2$ steps. Each solution for the neutrino momenta, including their fourfold ambiguity, are weighted by the SM expectation. The solution with the highest weight is retained and the corresponding top mass distribution is shown in Fig. 2. A simple Gaussian fit based mass estimator yields a statistical uncertainty of $1.5\,\mathrm{GeV}/c^2$ for $1\,\mathrm{fb}^{-1}$, with $10\,\mathrm{fb}^{-1}$ this will be reduced to $0.5\,\mathrm{GeV}/c^2$.

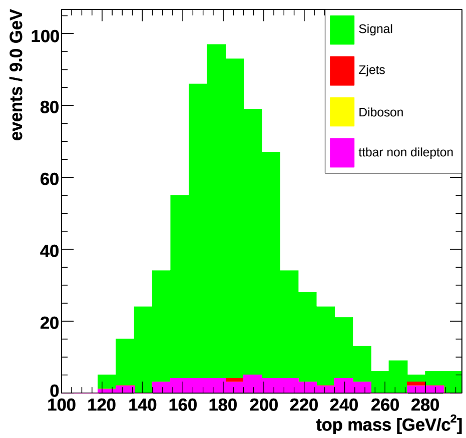

Fig. 2. Most likely top mass after selection for $1\,\mathrm{fb}^{-1}$.

The main systematic effect in this decay channel is the uncertainty on the jet energy scale, its effect on this measurement is $2.9\,\mathrm{GeV}/c^2$ for 1–10 fb^{-1} of data. Further improvement in the knowledge of the jet energy scale after $10\,\mathrm{fb}^{-1}$ is expected to reduce this uncertainty to about $1\,\mathrm{GeV}/c^2$.

3. Semi-leptonic final states

The semi-leptonic channel offers an easily selectable final state with its leptonic decaying top, while allowing a full reconstruction of the hadronic decaying top. Thus it is traditionally referred to as the *golden channel* for measuring the top quark mass.

The full analysis, described in detail in [4], uses events passing the single-muon trigger, and then requiring at least one isolated muon with $p_\mathrm{T} > 20\,\mathrm{GeV}/c$. Selected events must also contain four non-overlapping leading jets with $E_\mathrm{T} > 30\,\mathrm{GeV}$, two of them b-tagged and the other two anti-b-tagged.

A likelihood variable L_signal, combining three kinematic observables (p_T of muon candidate, p_T of second muon candidate, minimal E_T among four leading jets), is transformed into a probability P_signal, and a cut $P_\mathrm{signal} > 0.8$ is applied. A second likelihood variable L_comb is constructed from several observables, described in [4], to choose the correct jet pairing to reconstruct the hadronic decaying top quark from three of the four selected jets. The jet combination with the largest L_{comb} value is taken as the best pairing. Transforming the likelihood into a probability P_{comb} and requiring $P_{\mathrm{comb}} > 0.5$ for selected events, yields a pairing efficiency of 81.6%. For each jet combination a kinematic fit with a W mass constraint is performed [5]. Only jet combinations with a fit probability $P_{\chi^2} > 0.2$ are taken into account, discarding events where none of the jet combination fulfils this criterion. The full selection is described in detail in Table I.

TABLE I

Selection cuts for the signal and considered background samples.

	Signal	Other $t\bar{t}$	W+4j	Wbb+2j	Wbb+3j	S/B
L1+HLT trigger	62.2%	5.30%	24.1%	8.35%	8.29%	0.74
Pre-selection	45.8%	2.68%	11.7%	3.94%	5.91%	1.10
4 jets $E_{\mathrm{T}} > 30\,\mathrm{GeV}$	25.4%	1.01%	4.1%	1.48%	3.37%	1.69
$p_{\mathrm{T}}^{\mathrm{lepton}} > 20\,\mathrm{GeV}/c$	24.8%	0.97%	3.9%	1.41%	3.14%	1.72
b-tag criteria	5.5%	0.21%	0.052%	0.47%	0.70%	3.73
No jet overlap	3.0%	0.11%	0.027%	0.25%	0.44%	3.87
P_{χ^2}-cut 20%	1.4%	0.039%	0.0097	0.061	0.07	5.3
P_{signal}-cut 80%	1.2%	0.025%	0.0085	0.052	0.05	6.8
P_{comb}-cut 50%	0.7%	0.013%	0.0036	0.013	0.	8.2
Scaled $\mathcal{L} = 1\,\mathrm{fb}^{-1}$	588	64	6	2	0	8.2

Three different mass estimators, described in [4], are used to extract the top mass from the kinematically fitted hadronic top, their results are compared in Table II.

TABLE II

Comparison of three different mass estimators for the kinematically fitted hadronic top in all selected events.

	Gaussian fit	Gaussian ideogram	Full scan ideogram
Bias (GeV/c^2)	-0.84 ± 0.59	-4.35 ± 0.54	-2.58 ± 0.31
Slope	0.86 ± 0.18	1.01 ± 0.16	1.01 ± 0.13
Pull	0.82	1.01	1.01
stat. for $1\,\mathrm{fb}^{-1}$ (GeV/c^2)	1.01	1.14	0.66
stat. for $10\,\mathrm{fb}^{-1}$ (GeV/c^2)	0.32	0.36	0.21

The full range of systematic effects has been investigated and Table III summarises and combines the systematic uncertainties on each of the top quark mass estimators.

TABLE III

Summary of the systematic uncertainties for the top mass determination in semi-leptonic $t\bar{t}$ final states.

Source	Standard selection: Gaussian fit Δm_t (GeV/c^2)	Standard selection: Gaussian ideogram Δm_t (GeV/c^2)	Standard selection: Full scan ideogram Δm_t (GeV/c^2)
Pile-up (5%)	0.32	0.23	0.21
Underlying event	0.50	0.35	0.25
Jet energy scale (1.5%)	2.90	1.05	0.96
Radiation (Λ_{QCD}, Q_0^2)	0.80	0.27	0.22
Fragmentation (Lund b, σ_q)	0.40	0.40	0.30
b-tagging (2%)	0.80	0.20	0.18
Background	0.30	0.25	0.25
Parton density functions	0.12	0.10	0.08
Total systematical uncertainty	3.21	1.27	1.13
Statistical uncertainty (10 fb^{-1})	0.32	0.36	0.21
Total uncertainty	3.23	1.32	1.15

4. Fully hadronic final states

The fully hadronic final state consists of four light-quark jets and two b-jets, and thus kinematics that can be fully reconstructed. However, it also suffers from a large background stemming from QCD multi-jet production, which makes the signal selection very challenging. Furthermore the number of jets in the final state is source of significant levels of combinatorial background.

The selection uses the inclusive jet trigger [6] and a special inclusive b-jet trigger [7]. Eventshape variables like centrality, aplanarity and non-leading jet total transverse energy ($\sum_3 E_{\mathrm{T}} = \sum E_{\mathrm{T}} - E_{\mathrm{T}}^{\mathrm{jet}\ 1} - E_{\mathrm{T}}^{\mathrm{jet}\ 2}$), are used to separate the signal from the multi-jet background. Table IV summarises this cut-based selection. Improved selections based on neural networks, already employed for the cross section measurement, are still being optimised for the mass measurement [2].

TABLE IV

Selection cuts for the signal and QCD background.

Selection	Requirement	$\sigma\epsilon$ [pb]	$\sigma\epsilon_{\rm QCD}$ [pb]	S/B
Before selection (PYTHIA LO)		225	25M	$1/10^5$
Trigger	HLT multi-jet+b-jet	38	11600	1/300
Event	$6 \leq N_{\rm jet} \leq 8$, $E_{\rm T} \geq 30\,{\rm GeV}$	15	930	1/60
	centrality ≥ 0.68	9.9	324	1/33
	aplanarity ≥ 0.024	9.0	251	1/28
	$\sum_3 E_{\rm T} \geq 148\,{\rm GeV}$	9.0	229	1/25
b-tagging	1 b-tag	8.6	148	1/17
	2 b-tag	6.0	54	1/9

In order to perform the correct jet pairing, a likelihood variable is constructed from the several kinematic and topological observables, documented in [2]. Taking for each event the pairing with the highest likelihood value yields a pairing efficiency of 68%.

A kinematic reconstruction of the top quarks is then straightforward and the resulting invariant mass distribution of the top quark, with the paired non-b-jets rescaled such that they yield the W mass, is shown in Fig. 3.

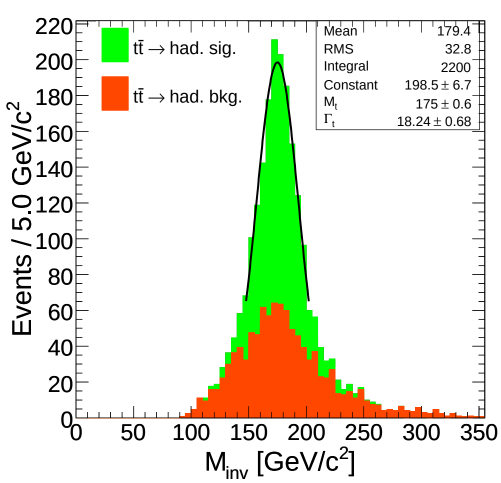

Fig. 3. Invariant mass distribution of the reconstructed and rescaled top for signal and combinatorial background with a Gaussian fit to the peak.

Already with $1\,\mathrm{fb}^{-1}$ of data the statistical error becomes negligible compared to the systematic uncertainties which are summarised in Table V. The S/B in the displayed mass window of Fig. 3 is about 2/3, although

TABLE V

Summary of the systematic uncertainties for the top mass determination in fully hadronic $t\bar{t}$ final states.

Source	Δm_t[GeV/c^2]
Pile up	0.4
Underlying event	0.6
PDF	1.4
IS/FS radiation	2.3
Fragmentation	0.9
Jet energy scale	2.3
b-tagging	0.3
Background	2.0

not shown since the currently available number of simulated events does not allow a determination of the QCD background shape and of the uncertainty it introduces into the top mass determination. Experience from CDF at the Tevatron [8, 9] indicates that this uncertainty can be understood at the $\sim 2\,\mathrm{GeV}/c^2$ level, when using data for background estimation.

5. Final states containing a J/Ψ meson

Top quark decays which include a J/Ψ meson can be used to determine the top mass through its correlation with the invariant mass of the reconstructed J/Ψ and the lepton from the W coming from the same top. The correlation is present because the reconstruction of the J/Ψ gives an accurate measurement of the b quark flight direction and momentum due to the relatively high mass of the meson. Details of the analysis can be found in [10].

While the three lepton final state allows a very clean experimental reconstruction, the main difficulty stems from the extremely low branching ratio (5.5×10^{-4}) for a $t\bar{t}$ event to decay into a final state with a leptonic J/Ψ, which yields only $\sim$4500 events per $10\,\mathrm{fb}^{-1}$.

Events are triggered using the inclusive lepton trigger with thresholds described in [6]. In events passing the trigger thresholds a J/Ψ candidate is constructed from two same-flavour, opposite-sign leptons with $2.8 < m_{\ell\ell} < 3.2\,\mathrm{GeV}/c^2$ and $2^\circ < \angle(\ell, \ell) < 35^\circ$. If a J/Ψ is found in an event, the isolated lepton with the highest p_{T} and higher than $40\,\mathrm{GeV}/c$ is considered as the lepton candidate from the W decay. Furthermore, for events with only one isolated lepton a cut $\sum_{\text{jets}} p_{\text{T}} > 100\,\text{GeV}/c$ is applied to suppress bosonic backgrounds, while for events with two isolated same-flavour leptons, a cut on the $[85, 97]\,\text{GeV}/c^2$ invariant mass range is used to suppress the Z-background. Table VI summarises the selection performance.

TABLE VI

Selection performance on signal and expected backgrounds. Channels are classified as signal (S), physics background (B) or combinatorial background (C).

Channel	BR$\cdot\sigma$ [fb]	$\epsilon_{\text{trigger}}$ [%]	ϵ_{select} [%]	Events in $10\,\text{fb}^{-1}$	Class
$t\bar{t} \to (b \to J/\Psi)\ell\nu - b\ell\nu$	107	93.9	15.7±0.4	158	S+C
$t\bar{t} \to (b \to J/\Psi)\ell\nu - b\tau\nu$	53	61.1	11.0±0.8	36	S
$t\bar{t} \to (b \to J/\Psi)\ell\nu - bqq$	320	55.3	10.9±0.3	193	S
$t\bar{t} \to (b \to J/\Psi)\tau\nu - b\ell\nu$	53	61.1	10.6±0.8	34	C
$t\bar{t} \to (b \to J/\Psi)\tau\nu - b\tau\nu$	27	14.2	2.8±1.2	1	B
$t\bar{t} \to (b \to J/\Psi)\tau\nu - bqq$	160	7.9	1.5±0.5	2	B
$t\bar{t} \to (b \to J/\Psi)qq - b\ell\nu$	320	55.3	10.7±0.3	190	C
$t\bar{t} \to (b \to J/\Psi)qq - b\tau\nu$	160	7.9	1.5±0.5	2	B
$t\bar{t} \to (b \to J/\Psi)qq - bqq$	959	0.1	0.2±0.5	0	B
$W + N\,\text{jets}, N > 1 \to J/\Psi X$	394	55.3	2.1±0.1	43	B
$Wb\bar{b} + \text{jets} \to J/\Psi X$	196	55.3	1.6±0.1	16	B
$Zb\bar{b} + \text{jets} \to J/\Psi X$	23	93.9	9.4±0.1	20	B
$b\bar{b} \to J/\Psi X$	1.3×10^9	$<2\cdot10^{-8}$	<1	<2.6	B

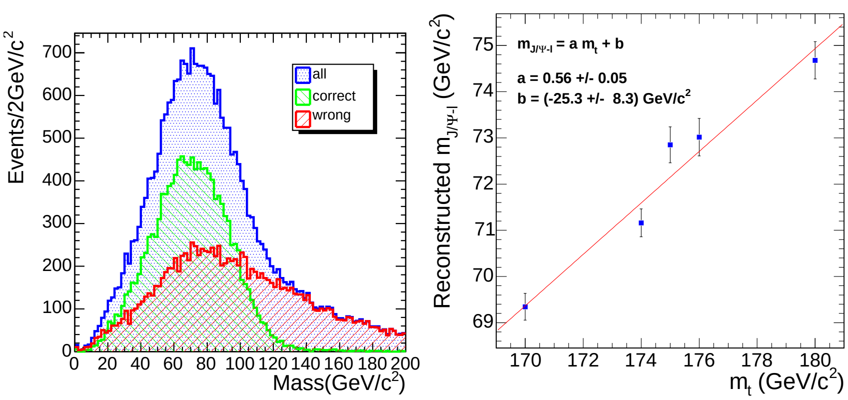

(a) (b)

Fig. 4. (a) Three-lepton invariant mass distribution for $m_t = 175\,\text{GeV}/c^2$ for selected events. (b) Correlation between the reconstructed three-lepton invariant mass and the input top mass.

Fig. 4(a) shows the three-lepton invariant mass in $t\bar{t}$ events after the selection. The fitted maximum is strongly correlated to the top mass which is shown in Fig. 4(b) for different input values.

The statistical uncertainty of this method is $1.2\,\mathrm{GeV}/c^2$ with $20\,\mathrm{fb}^{-1}$ of data and reaches $0.6\,\mathrm{GeV}/c^2$ with $50\,\mathrm{fb}^{-1}$. Table VII summarises the systematic uncertainties. This analysis reduces to a minimum those systematic uncertainties, like the jet energy scale and b-tagging, which dominate direct reconstruction top mass measurements.

TABLE VII

Summary of the systematic uncertainties for the top mass determination in J/Ψ final states.

Source	δm_t (GeV/c^2)	Source	δm_t (GeV/c^2)
Λ_{QCD}	0.31	Electron E scale	0.21
Q^2	0.56	Muon p scale	0.38
Scale definition	0.71	Electron E resolution	0.19
b-quark fragmentation	0.51	Muon p resolution	0.12
Light jet fragmentation	0.46	Jet E scale	0.05
Minimum bias/Underlying event	0.64	Jet E resolution	0.05
Proton PDF	0.28	Background knowledge	0.21
Total theoretical	1.37	Total experimental	0.54
		Total systematic	1.47

I would like to thank the organisers of the conference for the invitation and their hospitality and my CMS colleagues for providing results and information on their $t\bar{t}$ analyses.

REFERENCES

[1] R. Bonciani, S. Catani, M.L. Mangano, P. Nason, *Nucl. Phys.* **B529**, 424 (1998).

[2] M. Davids *et al.*, CMS Note, 2006/077 (2006), `http://cms.cern.ch/iCMS/jsp/openfile.jsp?tp=draft&files=2907_ttbar.pdf`

[3] Ch. Weiser, CMS Note, 2006/014 (2006), `http://cms.cern.ch/iCMS/jsp/openfile.jsp?type=NOTE& year=2006&files=NOTE2006_014.pdf`

[4] J. D'Hondt, J. Heyninck, S. Lowette. CMS Note, 2006/066 (2006), http://cms.cern.ch/iCMS/jsp/openfile.jsp?type=NOTE& year=2006& files=NOTE2006_066.pdf

[5] J. D'Hondt *et al.*, CMS NOTE, 2006/023 (2006).

[6] CMS Collaboration, CERN/LHCC, 2002-26 (2006), http://doc.cern.ch//archive/electronic/other/generic/public/cer-2336481.pdf, CMS TDR 6.2.

[7] M. Vos, F. Palla, CMS Note, 2006-030 (2006), http://cmsdoc.cern.ch/documents/06/note06_030.pdf

[8] F. Abe *et al.*, *Phys. Rev. Lett.* **79**, 1992 (1997).

[9] Combination of CDF and DØ results on the mass of the top quark, 2006.

[10] R. Chierici, A. Dierlamm, CMS Note, 2006-058 (2006), http://cmsdoc.cern.ch/documents/06/note06_058.pdf